

Catalytic transport of molecular cargo using diffusive binding along a polymer track

Lifei Zheng^{1,8*}, Hui Zhao^{1,2,8}, Yanxiao Han^{3,8}, Haibin Qian¹, Lela Vukovic⁴, Jasmin Mecinović^{1,7}, Petr Král^{3,5,6} and Wilhelm T. S. Huck^{1*}

Transport at the molecular scale is a prerequisite for the development of future molecular factories. Here, we have designed oligoanionic molecular sliders on polycationic tracks that exploit Brownian motion and diffusive binding to transport cargo without using a chemical fuel. The presence of the polymer tracks increases the rate of bimolecular reactions between modified sliders by over two orders of magnitude. Molecular dynamics simulations showed that the sliders not only diffuse, but also jump and hop surprisingly efficiently along polymer tracks. Inspired by acetyl-coenzyme A transporting and delivering acetyl groups in many essential biochemical processes, we developed a new and unconventional type of catalytic transport involving sliders (including coenzyme A) picking up, transporting and selectively delivering molecular cargo. Furthermore, we show that the concept of diffusive binding can also be utilized for the spatially controlled transport of chemical groups across gels. This work represents a new concept for designing functional nanosystems based on random Brownian motion.

Adenosine triphosphate (ATP)-fueled transport of vesicles by motor proteins (such as kinesin and dynein) along microtubular tracks is one of the most impressive examples of how molecular machines convert chemical fuel into motion¹. Inspired by these natural systems, chemists have striven to develop artificial systems with similar capabilities, with the ultimate goal of developing molecular robotics and assembly lines^{2–6}. So far, most artificial systems have employed DNA architectures as programmable devices for the transportation of DNA strands⁷ or gold nanoparticles⁸. Very recently, the first examples of molecular cargo displacement were demonstrated. In these designs, either chemical^{9,10} or optical energy¹¹ was applied to stimulate motion and transport at the molecular scale. Although these mimetics of active transport offer precise control over the delivery of molecules, this type of transport requires the synthesis of complex molecules and is an energy-consuming process. In many biological systems, especially in prokaryotes, diffusive or passive transport can form a much simpler, yet effective alternative¹². Depending on the size of the cargo, the distance to be covered and the dimensionality of the system, diffusive transport can be just as fast as active transport without paying an energy penalty^{13,14}. Despite a number of impressive examples of molecular-scale walkers based on reversible supramolecular interactions or dynamic covalent bonds^{15–20}, a synthetic diffusive transport system capable of picking up, transporting and ultimately depositing molecular cargo is lacking.

We are inspired by the efficient sliding and hopping motion of proteins along polynucleotides, as this form of diffusive transport does not require a chemical fuel^{21–24}. Sliding relies on multiple binding sites along the polynucleotide tracks, enabling the so-called diffusive binding. Diffusive binding is a type of non-covalent interaction where a small molecule can sample multiple binding sites that are spaced closely together and are similar in binding energy²⁵. Binding

to the different binding sites occurs without the molecules completely dissociating (that is, diffusing away) from one another. Such a situation has also been reported at solid surfaces¹⁵ or, for example, in binding of ligands to proteins²⁶. We have designed molecular sliders that bind to polymeric tracks via electrostatic interactions (Fig. 1). As shown below, these sliders not only diffuse along the tracks, but also have the capacity to ‘jump’ or ‘hop’ between tracks. Hopping involves temporary dissociation between sliders and tracks, enabling short periods in which 3D diffusion can take place before the sliders rebound to the tracks (either the same track, or a different one)²⁷. By functionalizing the molecular sliders with different reactive groups, we can study the changes in reaction rates between freely diffusing molecules and systems with reduced dimensionality. Furthermore, we show how the system can be designed such that the transport itself can be catalytic, as sliders can carry out multiple rounds of picking up, transporting and depositing functional groups.

Results

Constructing the slider–track system. Key to our design are transport molecules that bind diffusively onto polymer tracks. Ion pairing is one of the most fundamental interactions in biology and is also crucial in the sliding of proteins along polynucleotides^{21–24}. We hypothesized that diffusive binding might be a general principle regardless of the molecular details of the interacting species. Therefore, we designed a slider–track system consisting of oppositely charged species, in this case oligoanionic small molecules sliding along polycationic tracks. As shown in Fig. 1, coenzyme A (slider 1) and slider 2, containing three glutamic acids, were chosen as molecular sliders, while positively charged polyarginine (pArg) and polylysine (pLys) were employed as polymeric tracks. Importantly, both sliders carry a reactive thiol group that can be used for further functionalization with molecular cargo.

¹Radboud University, Institute for Molecules and Materials, Nijmegen, The Netherlands. ²Institute of Fundamental and Frontier Sciences (IFFS), University of Electronic Science and Technology of China (UESTC), Chengdu, China. ³Department of Chemistry, University of Illinois at Chicago, Chicago, IL, USA.

⁴Department of Chemistry and Biochemistry, University of Texas at El Paso, El Paso, TX, USA. ⁵Department of Physics, University of Illinois at Chicago, Chicago, IL, USA. ⁶Department of Biopharmaceutical Sciences, University of Illinois at Chicago, Chicago, IL, USA. ⁷Present address: Department of Physics, Chemistry and Pharmacy, University of Southern Denmark, Campusvej 55, Odense, Denmark. ⁸These authors contributed equally: Lifei Zheng, Hui Zhao and Yanxiao Han. *e-mail: zhenglifei0926@gmail.com; w.huck@science.ru.nl

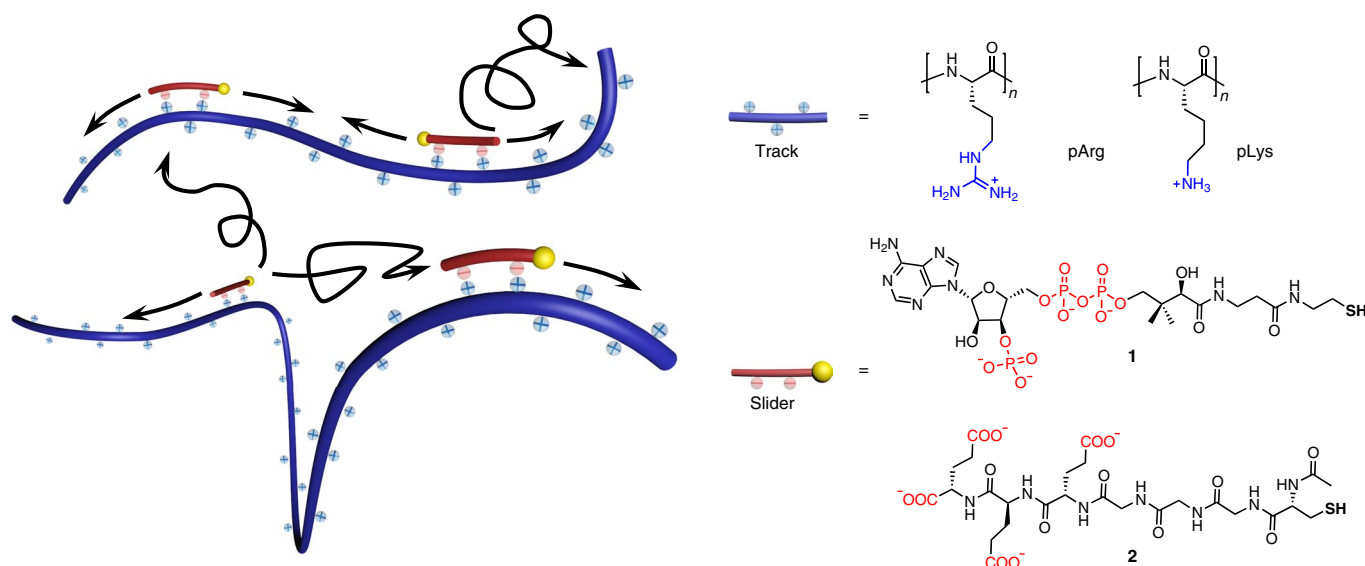


Fig. 1 | Schematic representation of the slider-track system. Molecular sliders bind diffusively onto polymer tracks via electrostatic interactions. These sliders not only slide along the tracks, but also have the capacity to ‘jump’ or ‘hop’ between tracks. Therefore, they can sample multiple binding sites that are spaced closely together on tracks, enabling efficient searching processes with reduced dimensionality. Oligoanions (sliders **1** and **2**) were chosen as molecular sliders, and polycations (pArg and pLys) were used as polymeric tracks. Reactive thiol functionalities are highlighted as yellow points for further functionalization.

Table 1 | Thermodynamic parameters for binding of sliders to tracks

	pArg with slider 1	pArg with slider 2	pLys with slider 1	pLys with slider 2
N (sites)	3.4 ± 0.05	3.2 ± 0.2	2.7 ± 0.1	2.9 ± 0.01
K_d (μM)	7.2 ± 0.3	1.3 ± 0.1	37 ± 3	5.2 ± 0.3
ΔH° (kcal mol ⁻¹)	-1.5 ± 0.02	-0.5 ± 0.01	-0.1 ± 0.01	0.4 ± 0.2
$T\Delta S^\circ$ (kcal mol ⁻¹)	5.6 ± 0.02	7.5 ± 0.03	5.9 ± 0.1	7.7 ± 0.1

We used isothermal titration calorimetry (ITC) to determine binding constants between the sliders and pArg ($M_w = 15\text{--}70$ kDa, 70–360 of Arg) or pLys ($M_w = 15\text{--}30$ kDa, 90–180 of Lys). The integrated heats from the raw ITC titration curves were fitted to a one-binding site model by assuming a single type of binding site on the polymer (Supplementary Section 2). Table 1 summarizes the thermodynamic parameters calculated from the ITC data: both sliders occupy around three charged monomer units of pArg and pLys. In accordance with the highly charged nature of the binding partners that contributes to energetically favourable electrostatic interactions, we found that slider 1 bound rather strongly to both polymer tracks, with $K_{d(\text{pArg}/\text{slider 1})} = 7.2\ \mu\text{M}$ and $K_{d(\text{pLys}/\text{slider 1})} = 37\ \mu\text{M}$. Slider 2 bound slightly more strongly than slider 1, with $K_d = 1.3\ \mu\text{M}$ for binding to pArg and $5.2\ \mu\text{M}$ for binding to pLys. It is worth noting that the measured dissociation constants represent the charged monomer concentrations of the respective tracks. The interactions between sliders and polycations appeared to be mainly driven by entropy, probably partially as a result of the release of chloride counterions on binding, which is consistent with an ion-pairing process²⁸. The electrostatic nature of binding was further supported by the substantial dependence of slider-polymer binding affinity on the concentration of sodium chloride (NaCl) in the buffer (Supplementary Fig. 2 and Supplementary Table 1).

Next, we investigated how diffusive binding of chemically charged sliders can greatly enhance the reaction kinetics between

sliders when they are bound to tracks. As a model reaction, we chose the reaction between an alkylthiol and bromo-substituted *N*-methylmaleimide, which yields a fluorescent product on substitution of the bromide by the thiolate (Fig. 2a). This reaction is typically slow in the absence of tracks, as seen in Fig. 2b,c, where μM concentrations of reactants (6 μM thiols and 5 μM maleimides, respectively) were used. However, following the addition of polycations, the reaction rates were enhanced significantly, with either slider reaching nearly full conversion within minutes on both pLys and pArg tracks (Fig. 2b,c). The concentrations of pArg and pLys were chosen such that the charged monomer concentration equivalents were 1.76 mM; that is, the concentration of positive charges on the track was at least 50-fold greater than the measured dissociation constants between polymers and sliders. It follows that over 98% of the reactants are bound on the polycations (at the μM concentrations used). We calculated the relative rate enhancements from the initial slopes of the reactions (Supplementary Table 2). The reaction between slider 1 and the bromo-substituted *N*-methylmaleimide-1 conjugate was accelerated by 113- and 110-fold by pArg and pLys, respectively. Similarly, slider 2 gave enhancements of 149- and 77-fold by pArg and pLys, respectively. As a control, the addition of 1.76 mM arginine (the same concentration of opposite charge, but no polymeric backbone) showed only a marginal increase in the reaction rate (Supplementary Figs. 25 and 26), confirming the essential role of the polymeric ‘tracks’ in increasing the rates of bimolecular reactions. The dependence of the rate enhancement on the NaCl concentration in the buffer further confirms the ion-pairing interactions between sliders and tracks (Supplementary Fig. 30). It is possible to tune the strength of the interaction between slider and track by altering the number of charges on the slider. We synthesized derivatives of slider 2 (Glu3) with one and five glutamic acid residues, instead of the three residues (Supplementary Section 3.5); these sliders show weaker ($K_{d(\text{pArg}/\text{Glu1})} = 440\ \mu\text{M}$) and stronger ($K_{d(\text{pArg}/\text{Glu5})} = 0.28\ \mu\text{M}$) binding to the tracks, respectively. Figure 2d shows the difference in reaction rate enhancements for sliders with different numbers of Glu residues, in the presence of 100 mM NaCl. Clearly, there is a trade-off in binding strength and reaction rate increase, with Glu3 performing optimally, and Glu1 and Glu5 binding

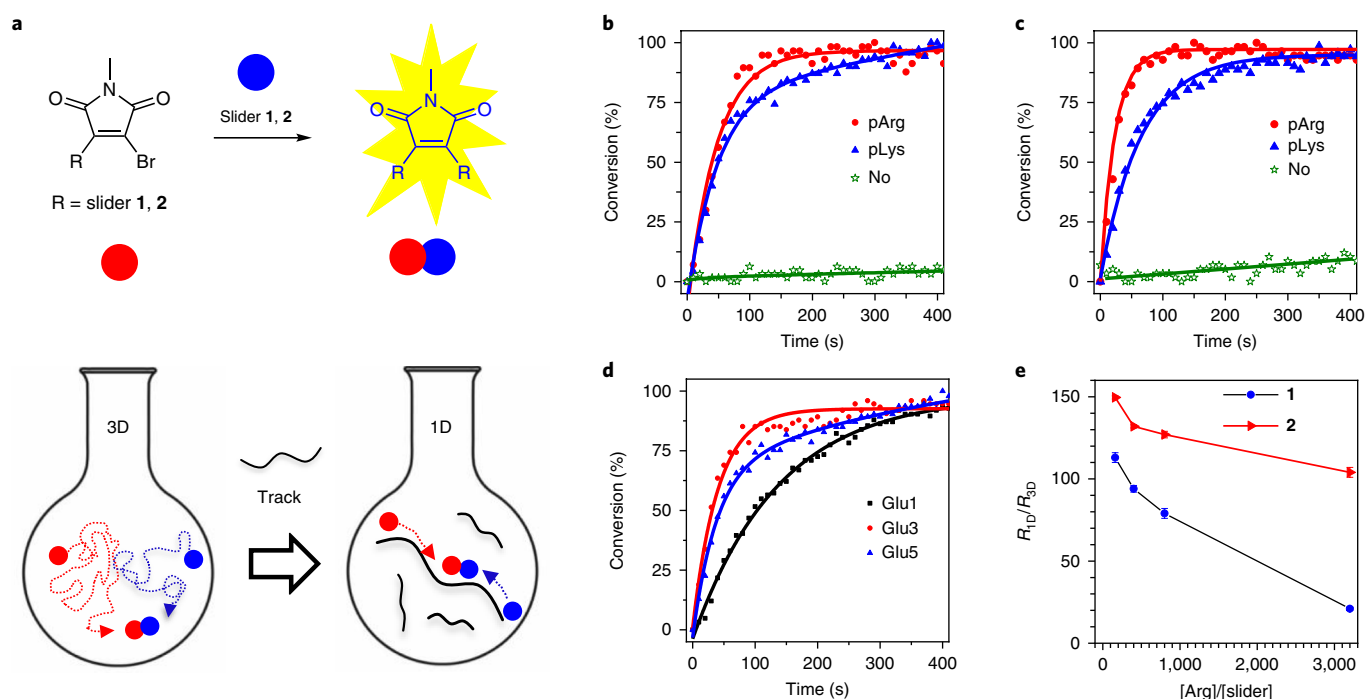


Fig. 2 | Kinetics studies of fluorogenic reactions between chemically charged sliders. **a**, Schematic representation of the reaction between a slider (blue dots) and a modified fluorogenic slider (red dots) in the absence or presence of polymeric tracks. Diffusive binding can greatly enhance reaction kinetics between chemically charged sliders when they are bound to tracks, demonstrating its potential in increasing the effective molarity of reactants by reducing the dimensionality of the system. **b**, The kinetics of the reaction between slider 1 and bromo-substituted *N*-methylmaleimide-1 are accelerated significantly by the presence of polycations. **c**, The kinetics of reaction between slider 2 and bromo-substituted *N*-methylmaleimide-2 are also accelerated significantly by the presence of polycations. **d**, Glu1, Glu3 (slider 2) and Glu5 reacting with bromo-substituted *N*-methylmaleimide-2 in the presence of pArg (N_{Arg} versus N_{slider} ratio of 160; 100 mM NaCl). Shown is a trade-off in binding strength and reaction rate increase, with Glu3 performing optimally. **e**, The rate R acceleration of the substitution reaction based on slider 1 decreases on increasing the concentration of pArg, in contrast to slider 2 showed a much weaker dependence on the concentration of pArg.

either too weakly (Glu1) or too strongly (Glu5). These results are fully consistent with ion-pairing interactions and diffusive binding between sliders and tracks.

The large excess (160-fold) of possible binding sites on the polymers makes it statistically highly unlikely that the reactants bind to neighbouring monomers on the chain. The starting positions of the sliders can be spaced apart even further by increasing the excess of binding sites from 160 to 3,200. Although the acceleration of the substitution reaction based on slider 1 decreased on increasing the concentration of pArg (Supplementary Fig. 27a), even at a ratio as high as 3,200, a 20-fold rate acceleration was still observed (Fig. 2e, blue line). Interestingly, slider 2 showed a much weaker dependence on the concentration of pArg (Supplementary Fig. 27b and red line in Fig. 2e). At the highest ratio of 3,200, the sliders bind to different tracks, yet the reaction rate still shows a 100-fold increase, thus strongly indicating that sliders can hop between tracks, because diffusion along the tracks alone should lead to a decrease in the reaction rate. Taken together, these results demonstrate the principle of diffusive binding, and its potential of reducing the dimensionality of the system and hence increasing the effective molarity of reactants^{29–31}.

Molecular dynamic simulations of sliders on polycationic tracks.

To obtain better insight into the nature of the interactions between the sliders and polymeric tracks, and their contributions to the observed rate acceleration of fluorogenic reactions, we carried out atomistic molecular dynamics (MD) simulations of the diffusion of the molecular sliders on polycation tracks (Supplementary Section 4).

The following cases were simulated: slider 1–pArg/pLys, with one slider 1 on one pArg/pLys track of 95 arginine/lysine residues; slider 2–pArg/pLys, with one slider 2 on one pArg/pLys track of 95 arginine/lysine residues and one slider 2 interacting with two short pLys tracks (25 and 29 residues long). All systems were placed in MES/MOPS buffer solutions. To quantify the folding or looping of each track, the radius of gyration (R_g) of the track and the hydrogen bonds within the track were calculated (Supplementary Figs. 34 and 35).

Figure 3a shows an example of 200 ns trajectories of slider 2 diffusing on a pArg track (for other combinations, see Supplementary Figs. 31–33). The sliders indeed form the expected ion pairs between the negatively charged carboxylate/phosphate residues on the sliders, and positively charged guanidinium/ammonium groups on the polymer tracks (Fig. 3a, inset). We found that both sliders show diffusive motion along the polycationic chain of pArg and pLys. At the same time, the simulation snapshots show that both sliders can induce the formation of transient loops on the tracks by attracting the track with oppositely charged groups of sliders. MD trajectories show that loops can be formed more easily on the pArg tracks than on pLys tracks (because of better coupling between the charged groups of the sliders and the track). Supplementary Fig. 34a shows that, during the 150–200 ns simulations, $R_g = 12/39 \text{ \AA}$ for slider 1/2–pArg, and $R_g = 45/55 \text{ \AA}$ for slider 1/2–pLys. R_g is smaller for pArg in the presence of both sliders, especially slider 1, indicating that the pArg chains are more condensed than pLys chains, which increases their intra-track connection and a one-dimensional (1D) diffusion of the attached sliders (switching between different loops). Supplementary Fig. 34b shows, for both sliders, that pArg

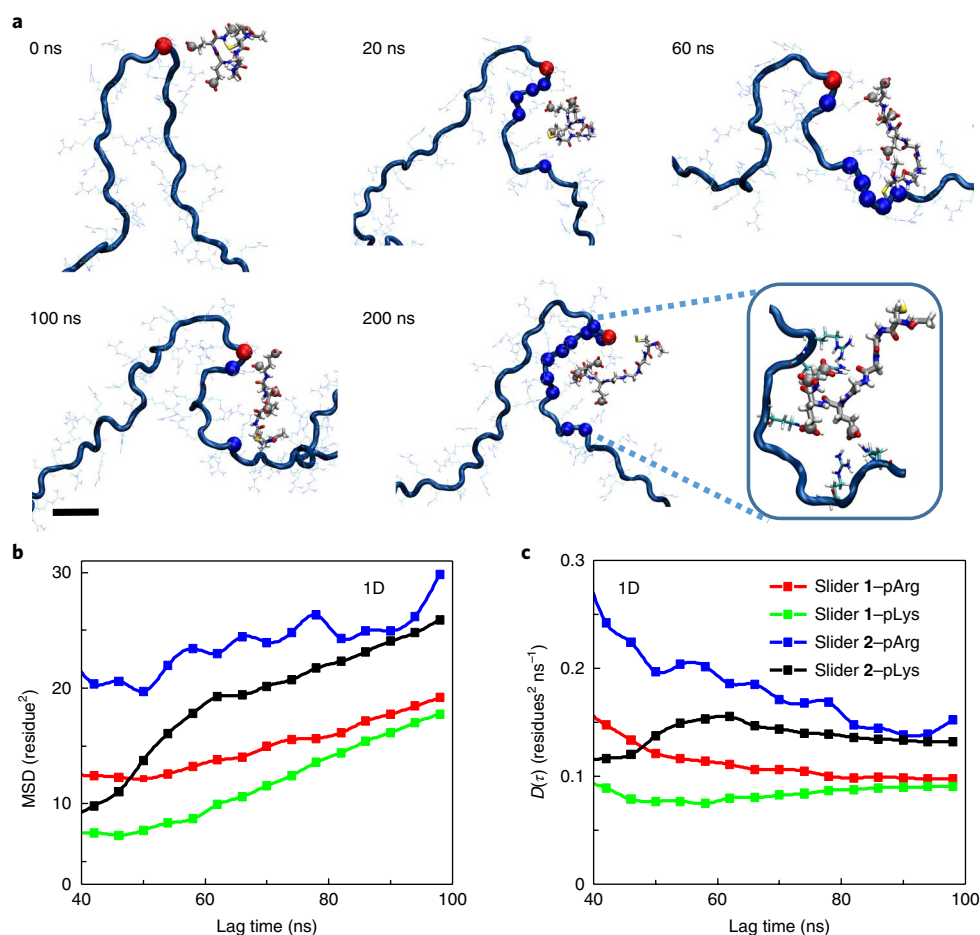


Fig. 3 | MD simulations of sliders on polycationic tracks. a, Slider 2 on the pArg track. The track is shown in dark blue with side chains, and the slider is shown in grey, with the C atom of the carboxyl group as a sphere, O in red, N in blue, S in yellow and H in white. The red point on the track is the initial nearest backbone atom from track to slider, and blue points are backbone atoms within 7 Å of the slider during the simulation. Scale bar, 1 nm. Inset, interactions between the negatively charged carboxylates and the positively charged guanidinium ion. **b,c**, Mean squared displacement and diffusion coefficient $D(\tau)$ for 1D diffusion of sliders along tracks. The 1D diffusion constants are larger on pArg than on pLys. Moreover, slider 2, with separate charged groups, shows higher mobility on both tracks.

has at least four times more hydrogen bonds within the track than pLys. The increased number of hydrogen bonds also indicates a higher chance of looping in the pArg track.

Next, we investigated whether the looping of pArg/pLys tracks is autonomous or is caused by the sliders. In the absence of sliders, after 60 ns of simulations both tracks are curved in a PPII helix form, but pArg still has almost four times more hydrogen bonds than pLys (Supplementary Fig. 35). However, the number of hydrogen bonds is smaller than in the presence of sliders. Therefore, pArg has a higher tendency of looping than pLys, and this looping tendency is further increased in the presence of sliders. The conformational changes in the polymer track could easily lead to oligoanions bridging ‘loops’ in the track, thereby significantly increasing the effective diffusion along the chain.

More importantly, it is highly likely that hopping between tracks also occurs. To verify this proposition, we also simulated the system of slider 2 interacting with two short pLys tracks (Supplementary Fig. 36). Initially, slider 2 was placed between the two tracks, as shown in the snapshot at 0 ns. After 18 ns interaction with both tracks, slider 2 dissociates from one track and completely binds to the other nearby track at 22 ns. The unbinding of slider 2 from one track was observed at 44 ns, which is the only unbinding event observed during the 0.9 μs simulation.

The dissociated slider finally jumped back to the original track at 46 ns. This simulation suggests that sliders indeed readily hop between tracks.

To understand better the interaction of sliders on a polycationic track, we calculated the Gibbs free energy of binding of slider 1/2 to the pArg track. Compared with experimental free energy values $-7.1/-8.0$ kcal mol⁻¹ (Table 1), the calculated values $(-4.9/-5.1$ kcal mol⁻¹) are smaller for slider 1/2-pArg, which may be due to the insufficient sampling and the restraints on the pArg. Based on the calculated potential of mean force, the energy barrier for slider 1/2 unbinding is estimated to be $\sim 5.6/5.8$ kcal mol⁻¹ (Supplementary Fig. 37). According to the Arrhenius equation and a method used in the literature³², this gives us an estimate of the slider 1 unbinding rate of 1.54×10^6 s⁻¹ and a binding time on pArg of 0.6 μs (assuming an Arrhenius frequency factor of 2.5×10^{10} s⁻¹). Similarly, the binding time of slider 2 is estimated to be 0.7 μs. This result implies that under the experimental conditions with high track concentrations there were numerous short searching events. A picture thus emerges where sliders make many small steps (slide) along the tracks in combination with larger displacements (jump and hop). This high mobility, in combination with close proximity to the tracks at all times, ensures very efficient encounters between the reactants, thus providing valuable theoretical support for our experimentally

observed rate accelerations of bimolecular reactions in the presence of polymeric tracks (vide supra).

To examine the diffusion of sliders further, mean squared displacements (MSDs) of sliders were computed from the trajectories at a variety of lag times (τ). A diffusion coefficient $D(\tau)$ was computed from $D(\tau) = \text{MSD}(\tau)/2E\tau$ (ref. 33), where E is the integer dimensionality of the system (1D along the tracks, using the coordinates of charged groups within each slider). To extract the 1D slider diffusion along the track, we find the backbone atom and its residue number nearest to the charge group centre of each slider. By using this residue number as the coordinate, we study 1D diffusion along the track and calculate MSD in the residue² (Fig. 3b) and $D(\tau)$ in the residue² per ns (Fig. 3c). Note that the calculated 1D diffusion rates incorporate jumping of the slider between bent loops of pLys and pArg. The 1D diffusion constants are larger on pArg than on pLys, which is consistent with their spontaneous looping (Supplementary Fig. 35). Moreover, slider 2, with separate charged groups, shows higher mobility on the tracks, suggesting that the structures of both the tracks and sliders can influence the 1D diffusion. Not only do the simulations provide a detailed insight into how bound sliders can diffuse along either track, they also show that the sliders most probably hop or jump along the polycationic tracks by locally distorting the backbone. The trends in the 1D diffusion of sliders are also in excellent agreement with the enhancement of the reaction rates observed in the experiments (for example, reactions involving slider 2 were enhanced 149-fold on pArg and 77-fold on pLys).

Inter-track molecular cargo transport. With the binding, sliding and hopping of sliders along polycationic tracks firmly established, we then wished to exploit this molecular system to shuttle molecular cargo along tracks. We were very much inspired by the biological function of coenzyme A derivatives to transfer acetyl- and other acyl groups³⁴. In our design, shown in Fig. 4a, the sliders adopt a very similar role in the transfer of molecular cargo between two types of monodisperse polyarginine track (Arg₁₈-S-acetyl/Arg₁₈-S-alkyne and Arg₂₀-Cys): in the first step, the sliders search and pick up the chemical group (cargo) from the end of donor tracks via a reversible thioester exchange reaction to form acylated sliders; subsequently, diffusive binding and hopping enables movement of the acylated sliders onto another Arg₂₀-Cys track. Once the sliders reach the reactive chain end, an irreversible native chemical ligation reaction ensures delivery of the cargo, and regeneration of the free sliders. Continued sliding and hopping can now restart the cycle when the slider picks up a new chemical group from Arg₁₈-S-acetyl or Arg₁₈-S-alkyne.

The starting tracks were obtained by reacting Arg₁₈-SH (synthesized by solid-phase peptide synthesis) with the corresponding *N*-hydroxysuccinimide esters, and were then characterized by matrix-assisted laser desorption/ionization–time-of-flight mass spectrometry (MALDI–TOF MS) (Supplementary Section 5.1). It is necessary to point out that the Arg₁₈-S-acetyl and Arg₁₈-S-alkyne contained ~7% and ~25% of the starting material Arg₁₈-SH, respectively, which could not be separated by high-performance liquid chromatography.

We first studied the reactivity of thioester exchange between slider 1 (10 μ M, M_w 767) and Arg₁₈-S-acetyl (10 μ M, M_w 3,015) in MOPS buffer (10 mM, pH 7.1) using MALDI–TOF MS. After 1 h, the acetyl transfer was complete, and two new peaks appeared corresponding to Acetyl-1 (M_w 809) and Arg₁₈-SH (M_w 2,973) (Supplementary Fig. 42). Next, we followed the native chemical ligation reaction between acetyl-1 (10 μ M) and Arg₂₀-Cys (10 μ M, M_w 3,244) in the same buffer. The MALDI–TOF MS spectrum showed nearly full conversion of Arg₂₀-Cys into Arg₂₀-acetylCys (M_w 3,286) within 1 h (Supplementary Fig. 43).

Subsequently, we combined all processes by adding sliders into the mixture of Arg₁₈-S-acetyl (10 μ M) and Arg₂₀-Cys (5 μ M) in the presence of tris(3-hydroxypropyl)phosphine (THPP, 200 μ M),

which prevented disulfide bond formation between the free thiols in the mixture. The reaction mixtures were analysed by MALDI–TOF MS at various time points. Due to the structural similarity of Arg₂₀-Cys and Arg₂₀-S-acetyl, we estimated transfer efficiencies at different time points from the integrations of their corresponding peaks in the mass spectra (Fig. 4b), in which the ratio of the product peak to that of the starting track increased over time, proving that the acetyl group was transferred from one track to another. Figure 4c,d (blue lines) shows that acetyl transfer by 1 μ M slider 1 reaches ~55% conversion within 1 h, while over the same time period 1 μ M slider 2 deposited 80% of the acetyl group on the second track. Increasing the loading amount of sliders to stoichiometric amounts significantly accelerated the acetyl transfer from one track to another, and also slightly enhanced the conversions (Fig. 4c,d, red lines). Decreasing the ratio of slider to polymer track to 5% obviously reduced the transfer rate, but, surprisingly, a conversion of 85% after 3 h was still achieved in the case of slider 2 (Fig. 4d, black line) and 60% for slider 1 (Fig. 4c, black line). This result means that each slider 2 molecule has, on average, carried out transfer of the acetyl group over ten times, making this the first example of a catalytic transfer process. A series of control experiments were performed to confirm the role of sliders as molecular transporters. As shown in Fig. 4c,d (yellow lines), in the absence of sliders, but presence of THPP, acetyl transfer only occurred to a small extent (~12% in 4 h) after mixing Arg₁₈-S-acetyl with Arg₂₀-Cys. The addition of 5% ATP (a possible slider, but not capable of picking up cargo) gave a slight enhancement of the background reaction (Supplementary Fig. 46). These controls show that the acetyl transfer is not a result of direct reaction between the tracks. The addition of non-charged acetyl cysteamine (Ac-cysteamine) into the mixture had no effect on the molecular transfer (Fig. 4e, yellow line). Interestingly, slider 2 (Fig. 4e, red line) was a more effective catalyst than both the weaker binder Glu1 (blue line) and the stronger binder Glu5 (pink line), an observation that suggests a certain balance of binding versus diffusing in this process; that is, the association needs to be strong enough to bind the sliders to the tracks, but also weak enough to allow fast diffusion along the tracks. A final control experiment was performed by studying the catalytic acetyl transfer between two short oligoarginines (Arg₃-S-acetyl and Arg₄-Cys) to further illustrate the relevance of diffusive binding on the catalytic process. To reach the same overall concentration of positive charges compared to that with long tracks, a certain amount of Arg₅ oligomer without any reactive groups was added. Such tracks would still allow binding of the sliders, but no sliding can occur because their sizes are comparable to each other. Under identical experimental conditions, the presence of 20% slider 2 only gave a slight enhancement of the background reaction (Supplementary Fig. 48), confirming the importance of a 1D search based on diffusive binding of sliders that efficiently shuttle the molecular cargo along tracks.

Finally, we expanded the molecular cargo scope to include a clickable alkyne group by using Arg₁₈-S-alkyne as the donor track. It was shown that the alkyne group can be successfully transferred by slider 2 with high efficiency (~75% within 1 h) (Supplementary Fig. 49). To show that the transferred reactive group can bring additional value to the acceptor track, we synthesized an azide-bearing fluorogenic coumarin dye (Supplementary Section 5.5). The mass spectrum showed an additional 203 Da mass shift, demonstrating that it can be successfully hooked onto the alkyne-functionalized acceptor track, as also indicated by the fluorescence of the product (Supplementary Fig. 50).

In chemical terms, the catalytic transfer of cargo from one track to another represents an unusual case of a catalytic cycle. Conventional catalysts promote reactions by lowering the activation energy. In the current case, however, the transformation between two polymers was accelerated through a molecular shuttle mechanism^{35,36}, meaning that direct collisions between the two reactants

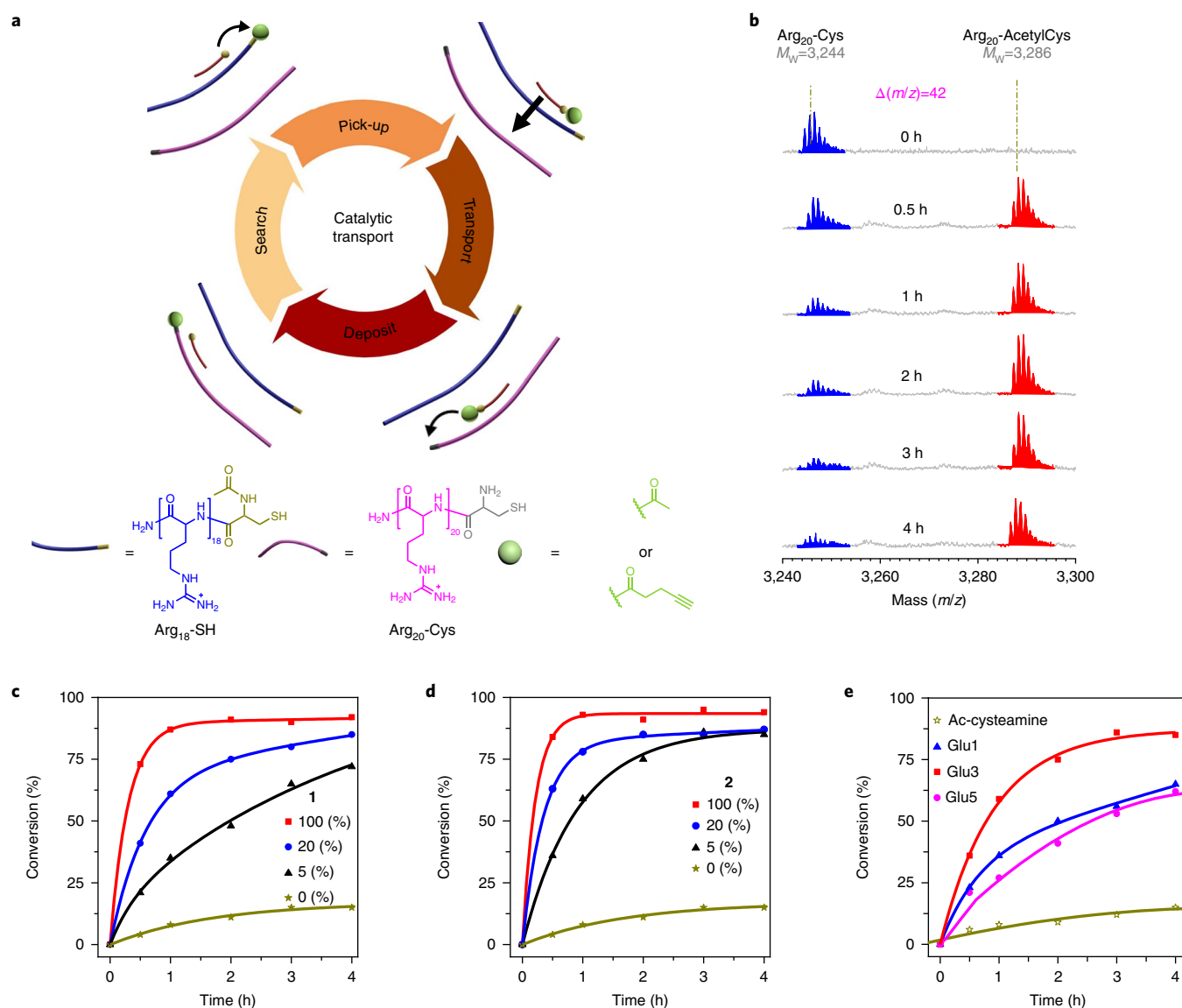


Fig. 4 | Inter-track molecular cargo transport. **a**, Schematic representation of the molecular transfer between Arg₁₈-S-acetyl/Arg₁₈-S-alkyne and Arg₂₀-Cys mediated by transporter slider 1/2. First, the sliders search and pick up the molecular cargo from donor tracks to form acylated sliders. Subsequently, diffusive binding and hopping can move acylated sliders onto another Arg₂₀-Cys track. Finally, an irreversible native chemical ligation reaction ensures deposition of the cargo, and regeneration of the free sliders. **b**, MALDI-TOF MS spectrum of the transport mixtures mediated by 1 μM (20%) slider 2 at various time points. The ratio of the product peak (Arg₂₀-S-acetyl) to that of the starting track (Arg₂₀-Cys) increased over time, indicating the occurrence of inter-track acetyl transfer. **c,d**, Transfer kinetics for 0, 5, 20 and 100% slider 1 and 2 (derived from mass spectra). Increasing the loading amount of the sliders not only accelerated the acetyl transfer from one track to another, but also slightly enhanced the conversions. **e**, Transfer kinetics using 5% Ac-cysteamine, Glu1, Glu3 and Glu5 (derived from mass spectra). The presence of non-charged Ac-cysteamine had no effect on the molecular transfer. Slider 2 was more effective than both the weaker binder Glu1 and the stronger binder Glu5.

were not necessarily needed. We anticipate that the introduction of click chemistry will significantly broaden the type of systems that can benefit from our catalytic transport principle.

Molecular cargo transport within physically separated compartments. Encouraged by the results of the inter-track molecular cargo transport in solution, we now wished to expand this central concept to the transport of chemical groups from donor tracks to acceptor tracks that are physically separated. In proof-of-concept experiments we demonstrate control over the localization and transport of molecules, which would be an important feature of future molecular nanosystems where communication between compartments can be used to create functions such as sensing, dissipative self-assembly or logic operations^{6,14,37}.

Our first step was the generation of a hydrogel that can non-covalently immobilize the pArg tracks. For this purpose, 0.2-mm-thick polyacrylamide (PAAm) hydrogels were prepared containing 2% carboxylate groups (compared to acrylamide monomers; see Supplementary Section 6.1 for details). Confocal microscopy was used to visualize the diffusion of Arg₁₈-S-coumarin (see Supplementary Fig. 51 for synthesis) inside hydrogels. Supplementary Movie 1 shows that in a trilayer system consisting of three 0.2-mm-thick gels loaded with 200 μM tracks (labelled or un-labelled), the Arg₁₈-S-coumarin in the central layer does not significantly diffuse into either the top or bottom gel over a time period of 2 h, indicating that the pArg tracks can be effectively compartmentalized within the slightly negatively charged PAAm hydrogels (nc-PAAm).

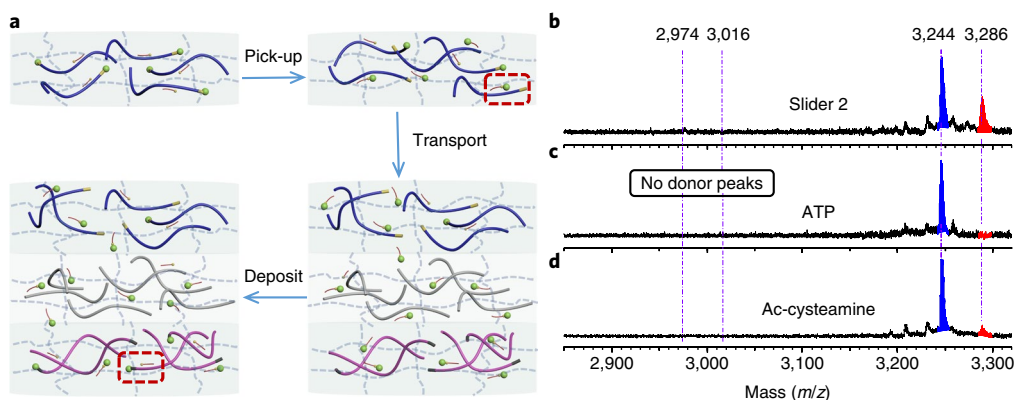


Fig. 5 | Molecular cargo transport within physically separated compartments. **a**, Schematic representation of slider-2-mediated molecular transport between Arg₁₈-S-acetyl and Arg₂₀-Cys, which are physically separated. A sandwich-type construct containing a filtering nc-PAAm layer was designed to prevent direct content mixing of donor and acceptor tracks, but still allow the sliders to diffuse through. Slider 2 was first introduced to the agarose hydrogel soaked with donor tracks. This gel was then placed on top of a bilayer gel consisting of 'filter' gel as a middle layer and a bottom layer with acceptor tracks in agarose gel. The delivery of cargo was allowed to proceed for 4 h. Red boxes indicate diffusive binding-mediated 1D searching for reactive sites on the tracks. **b–d**, MALDI-TOF MS spectra of the acceptor gel after 4 h incubation in the presence of slider 2, ATP and Ac-cysteamine, respectively. In these spectra, the absence of any donor track signal proves that transfer must have occurred via the sliders. ATP, without a free thiol group, showed no cargo transport at all. Acetyl transport across the immobilized track layer mediated by slider 2 was more efficient than that mediated by non-charged Ac-cysteamine, showing that the concept of diffusive binding can be used for the spatially controlled transport of functional groups.

Next, we studied the diffusion of sliders inside the gel matrix by wet stamping^{38,39}, during which the diffusive spreading of a fluorescently labelled slider (CoA-NBD) from an agarose stamp (2%) with 250- μm -wide microfabricated pillars into nc-PAAm hydrogels containing positively charged tracks was recorded from the bottom of gel at different time points. (Supplementary Section 6.3). Supplementary Fig. 53 shows the vertical cross-sections from each experimental micrograph of the bottom gel in time. As can be seen, the fluorescently labelled sliders spread rapidly in pArg loaded gels, and finally reach a homogeneous distribution over the bottom gel within ~ 15 min.

We now wish to repeat the transfer of functional groups not only between different tracks, but also between different locations. Using the native chemical ligation reaction between acetyl-1 and Arg₂₀-Cys as a model, we first studied the chemical reactivity within different hydrogels. In these experiments, 5 μl of 1 mM acetyl-1 was put on top of one piece of hydrogel (nc-PAAm or 2% agarose) soaked with 200 μM Arg₂₀-Cys, then dried by a gentle flow of argon for 30 s. These hydrogels were kept in argon for 1 h and then directly subjected to MALDI-TOF MS analysis. As shown in Supplementary Fig. 54, around 35% conversion of Arg₂₀-Cys into Arg₂₀-acetylCys was observed within the agarose gel; however, we did not observe any acetyl transfer within the nc-PAAm gel. This low reactivity might be due to the large steric effect when the reactive polymer ends were brought in close proximity to the gel backbone. Based on these observations, we designed a sandwich-type construct in which the donor tracks and acceptor tracks are placed in two agarose gels that allow reaction to occur. These gels are separated by a filtering nc-PAAm layer containing immobilized Arg₂₀ tracks, which prevents the direct content mixing of donor and acceptor tracks but still allows the sliders to diffuse through. As shown in Fig. 5a, we first introduced slider 2 (7.5 μl of 1 mM slider 2 solution) to the agarose hydrogel soaked with 300 μM Arg₁₈-S-acetyl. After allowing the sliders to pick up the cargo (2 h), we placed this gel on top of a bilayer gel consisting of 'filter' gel soaked with 200 μM Arg₂₀ tracks as the middle layer and a bottom layer with 200 μM Arg₂₀-Cys acceptor tracks in agarose gel. The delivery of cargo was allowed to proceed for 4 h, after which the bottom layer was analysed using MALDI-TOF MS. Figure 5b shows that $\sim 33\%$ of Arg₂₀-Cys tracks

have been converted into Arg₂₀-acetylCys. Importantly, the absence of any signal related to donor tracks (Arg₁₈-S-acetyl and Arg₁₈-SH) proves that transfer must have occurred via the sliders that transported the acetyl group across the immobilized track layer. A control experiment with charged ATP showed no conversion at all (Fig. 5c), further confirming that the acetyl transfer was mediated by sliders. As expected, in the presence of non-charged Ac-cysteamine, acetyl transport occurred, but only to a small extent ($\sim 9\%$ within 4 h, Fig. 5d). These results strongly suggest that the concept of diffusive binding can be used for the spatially controlled transport of functional groups.

Conclusions

We have presented examples of catalysis mediated by diffusive binding and hopping of a molecular slider that picks up, transports and deposits functional groups from one polymer track to another. Moreover, we have expanded this central concept to the transport of chemical groups that are localized in physically separated compartments. Our system is inspired by the efficient 1D Brownian motion of proteins along polynucleotides found in nature, but adapted to a generally applicable route for functional nanosystems. Interestingly, such systems would be entirely driven by the chemical reaction(s) taking place, as the transport mechanism itself is operating at thermodynamic equilibrium. In this context it is important to note that recent work on the dynamics of supramolecular polymers⁴⁰ has shown that monomer exchange in such systems involves 'surfing' of monomers along the fibre backbones at much higher rates compared to direct exchange into solution. This raises the prospect of designing future systems of supramolecular polymers with reactive monomers that carry their load along the self-assembled structures. We therefore anticipate that our work will inspire new applications based on Brownian motion, including reaction diffusion systems and other spatially encoded smart materials.

Methods

Standard procedure for fluorogenic reaction in the presence or absence of polycations. Bromo-substituted *N*-methyl-maleimide slider conjugates (2 μl of 250 μM) and various amounts of polycations were pre-mixed in 50 mM MES or MOPS buffer in the absence or presence of sodium chloride. The final volume of these mixtures was 98 μl . Then, 2.4 μl of freshly prepared slider solutions (250 μM

stock) were added and the reaction kinetics was immediately recorded on a real-time plate reader (excitation at 416 nm; emission at 600 nm).

Standard procedure for catalytic transfer reactions in solution. To a mixture of Arg₁₈-S-acetyl or Arg₁₈-S-alkyne (10 μM), Arg₂₀-Cys (5 μM) and THPP (200 μM) in MOPS buffer (10 mM, pH 7.1), an aliquot of a stock solution of slider (final concentrations varied from 0.25 μM to 5 μM) in water was added and the mixture was shaken on a Thermo-Shaker at 25 °C. At each time point, 2 μl of the reaction mixture was analysed by MALDI-TOF MS.

Standard procedure for molecular transport in gel. Two agarose gels (2%) were soaked with 300 μM Arg₁₈-S-acetyl and 200 μM Arg₂₀-Cys in MOPS buffer (10 mM, pH 7.1) with 1 mM THPP for 4 h, respectively. The donor gel was then treated with 7.5 μl of 1 mM slider 2 solution and kept under argon for 2 h. Afterwards, it was placed on top of a bilayer gel consisting of 'filter' gel soaked with 200 μM Arg₂₀ tracks as the middle layer and a bottom acceptor gel layer. The obtained sandwich-type construct was placed in a Petri dish containing argon and several pieces of wet cotton to prevent drying during the experiment. After 4 h, the bottom layer was directly analysed using MALDI-TOF MS.

A detailed description of all experimental procedures, full characterization of all compounds, as well as details of the MD simulations are provided in the Supplementary Information.

Data availability

The authors declare that all the data generated and analysed during this study are included within this Article and its Supplementary Information. The software and codes used to perform simulation and analysis are cited in the Article. The data sets are available from authors Y.H. and P.K. on reasonable request.

Received: 23 November 2017; Accepted: 4 December 2018;

Published online: 21 January 2019

References

- Shliwa, M. & Woehlke, G. Molecular motors. *Nature* **422**, 759–765 (2003).
- Kinbara, K. & Aida, T. Toward intelligent molecular machines: directed motions of biological and artificial molecules and assemblies. *Chem. Rev.* **105**, 1377–1400 (2005).
- Browne, W. R. & Feringa, B. L. Making molecular machines work. *Nat. Nanotech.* **1**, 25–35 (2006).
- Coskun, A., Banaszak, M., Astumian, R. D., Stoddart, J. F. & Grzybowski, B. A. Great expectations: can artificial molecular machines deliver on their promise? *Chem. Soc. Rev.* **41**, 19–30 (2012).
- Erbas-Cakmak, S., Leigh, D. A., McTernan, C. T. & Nussbaumer, A. L. Artificial molecular machines. *Chem. Rev.* **115**, 10081–10206 (2015).
- Grzybowski, B. A. & Huck, W. T. S. The nanotechnology of life-inspired systems. *Nat. Nanotech.* **11**, 585–592 (2016).
- Wickham, S. F. J. et al. Direct observation of stepwise movement of a synthetic molecular transporter. *Nat. Nanotech.* **6**, 166–169 (2011).
- Gu, H., Chao, J., Xiao, S. J. & Seeman, N. C. A proximity-based programmable DNA nanoscale assembly line. *Nature* **465**, 202–205 (2010).
- von Delius, M., Geertsema, E. M. & Leigh, D. A. A synthetic small molecule that can walk down a track. *Nat. Chem.* **2**, 96–101 (2010).
- Kassem, S., Lee, A. T. L., Leigh, D. A., Markevicius, A. & Solà, J. Pick-up, transport and release of a molecular cargo using a small-molecule robotic arm. *Nat. Chem.* **8**, 138–143 (2016).
- Chen, J., Wezenberg, S. J. & Feringa, B. L. Intramolecular transport of small-molecule cargo in a nanoscale device operated by light. *Chem. Commun.* **52**, 6765–6768 (2016).
- Soh, S., Byrka, M., Kandere-Grzybowska, K. & Grzybowski, B. A. Reaction-diffusion systems in intracellular molecular transport and control. *Angew. Chem. Int. Ed.* **49**, 4170–4198 (2010).
- Kopperger, E., Pirzer, T. & Simmel, F. C. Diffusive transport of molecular cargo tethered to a DNA origami platform. *Nano Lett.* **15**, 2693–2699 (2015).
- Thubagere, A. J. et al. A cargo-sorting DNA robot. *Science* **357**, 1112–1121 (2017).
- Perl, A. et al. Gradient-driven motion of multivalent ligand molecules along a surface functionalized with multiple receptors. *Nat. Chem.* **3**, 317–322 (2011).
- Pulcu, G. S., Mikhailova, E., Choi, L. S. & Bayley, H. Continuous observation of the stochastic motion of an individual small-molecule walker. *Nat. Nanotech.* **10**, 76–83 (2015).
- Campana, A. G. et al. A small molecule that walks non-directionally along a track without external intervention. *Angew. Chem. Int. Ed.* **51**, 5480–5483 (2012).
- Campana, A. G., Leigh, D. A. & Lewandowska, U. One-dimensional random walk of a synthetic small molecule toward a thermodynamic sink. *J. Am. Chem. Soc.* **135**, 8639–8645 (2013).
- Thordarson, P., Bijsterveld, E. J. A., Rowan, A. E. & Nolte, R. J. M. Epoxidation of polybutadiene by a topologically linked catalyst. *Nature* **424**, 915–918 (2003).
- van Dongen, S. F. M. et al. A clamp-like biohybrid catalyst for DNA oxidation. *Nat. Chem.* **5**, 945–951 (2013).

- Givaty, O. & Levy, Y. Protein sliding along DNA: dynamics and structural characterization. *J. Mol. Biol.* **385**, 1087–1097 (2009).
- Vuzman, D. & Levy, Y. DNA search efficiency is modulated by charge composition and distribution in the intrinsically disordered tail. *Proc. Natl Acad. Sci. USA* **107**, 21004–21009 (2010).
- Blainey, P. C. et al. Nonspecifically bound proteins spin while diffusing along DNA. *Nat. Struct. Mol. Biol.* **16**, 1224–1229 (2009).
- Mangel, W. F. et al. Molecular sled is an eleven-amino acid vehicle facilitating biochemical interactions via sliding components along DNA. *Nat. Commun.* **7**, 10202 (2016).
- Berg, O. G., Winter, R. B. & von Hippel, P. H. Diffusion-driven mechanisms of protein translocation on nucleic acids. 1. Models and theory. *Biochemistry* **20**, 6929–6948 (1981).
- Zhong, D., Douhal, A. & Zewail, A. H. Femtosecond studies of protein–ligand hydrophobic binding and dynamics: human serum albumin. *Proc. Natl Acad. Sci. USA* **97**, 14056–14061 (2000).
- Jeltsch, A. & Urbanke, C. in *Restriction Endonucleases* (ed. Pingoud, A. M.) 95–110 (Nucleic Acids and Molecular Biology series, Springer, Heidelberg, 2004).
- Ross, P. D. & Subramanian, S. Thermodynamics of protein association reactions: forces contributing to stability. *Biochemistry* **20**, 3096–3102 (1981).
- Turkin, A. et al. Speeding up biomolecular interactions by molecular sledding. *Chem. Sci.* **7**, 916–920 (2016).
- Xiong, K., Erwin, G. S., Ansari, A. Z. & Blainey, P. C. Sliding on DNA: from peptides to small molecules. *Angew. Chem. Int. Ed.* **55**, 15110–15114 (2016).
- Zhang, L. et al. Accelerating chemical reactions by molecular sledding. *Chem. Commun.* **53**, 6331–6334 (2017).
- Zhang, D., Gullingsrud, J. & McCammon, J. A. Potentials of mean force for acetylcholine unbinding from the α7 nicotinic acetylcholine receptor ligand-binding domain. *J. Am. Chem. Soc.* **128**, 3019–3026 (2006).
- Giorgino, T. *Computing Diffusion Coefficients in Macromolecular Simulations: The Diffusion Coefficient Tool for VMD* https://github.com/tonigi/vmd_diffusion_coefficient (2011).
- Elovson, J. & Vagelos, P. R. Acyl carrier protein. X. Acyl carrier protein synthetase. *J. Biol. Chem.* **243**, 3603–3611 (1968).
- Fang, X., Yu, P. & Morandi, B. Catalytic reversible alkene–nitrile interconversion through controllable transfer hydrocyanation. *Science* **351**, 832–836 (2016).
- Fang, X., Cacherat, B. & Morandi, B. CO- and HCl-free synthesis of acid chlorides from unsaturated hydrocarbons via shuttle catalysis. *Nat. Chem.* **9**, 1105–1109 (2017).
- Maiti, S., Fortunati, I., Ferrante, C., Scrimin, P. & Prins, L. J. Dissipative self-assembly of vesicular nanoreactors. *Nat. Chem.* **8**, 725–731 (2016).
- Campbell, C. J., Klajn, R., Fialkowski, M. & Grzybowski, B. A. One-step multilevel microfabrication by reaction–diffusion. *Langmuir* **21**, 418–423 (2005).
- Semenov, S. N., Markvoort, A. J., de Greef, T. F. A. & Huck, W. T. S. Threshold sensing through a synthetic enzymatic reaction–diffusion network. *Angew. Chem. Int. Ed.* **53**, 8066–8069 (2014).
- Bochicchio, D., Salvalaglio, M. & Pavan, G. M. Into the dynamics of supramolecular polymers at submolecular resolution. *Nat. Commun.* **8**, 147 (2017).

Acknowledgements

This work was supported by the Netherlands Organization for Scientific Research (NWO) TOPPUNT grant 718.014.001 (to W.T.S.H.), the Ministry of Education, Culture and Science (Gravity programme, 024.001.035, to W.T.S.H.), an NSF DMR-1506886 grant (to P.K.) and by start-up funding from the University of Texas at El Paso (to L.V.). H.Z. is a recipient of a Radboud Excellence Fellowship.

Author contributions

W.T.S.H. supervised the research. L.Z., H.Z. and W.T.S.H. planned the project and designed experiments. L.Z. and H.Z. synthesized and characterized all compounds. L.Z. and H.Z. performed kinetic studies of fluorogenic reactions and analysed data. L.Z. and H.Q. performed catalytic molecular transfer experiments and analysed data. L.Z. and J.M. analysed the ITC data. Y.H., L.V. and P.K. performed computational simulations. L.Z., Y.H., P.K. and W.T.S.H. wrote the manuscript.

Competing interests

The authors declare no competing interests.

Additional information

Supplementary information is available for this paper at <https://doi.org/10.1038/s41557-018-0204-7>.

Reprints and permissions information is available at www.nature.com/reprints.

Correspondence and requests for materials should be addressed to L.Z. or W.T.S.H.

Publisher's note: Springer Nature remains neutral with regard to jurisdictional claims in published maps and institutional affiliations.

© The Author(s), under exclusive licence to Springer Nature Limited 2019